

# Maximum Likelihood Estimation of Turbulence Spectrum Parameters

William D. Mark\*

*Bolt Beranek and Newman Inc., Cambridge, Massachusetts*

Estimation of the integral scale and intensity of a generic turbulence record is treated as a statistical problem of parameter estimation. Properties of parameter estimators and the method of maximum likelihood are reviewed. Likelihood equations are derived for estimation of the integral scale and intensity applicable to a general class of turbulence spectra that includes the von Kármán and Dryden transverse and longitudinal spectra as special cases. The method is extended to include the Bullen transverse and longitudinal spectra. Coefficients of variation are given for maximum likelihood estimates of the integral scale and intensity of the von Kármán spectra. Application of the method is illustrated by estimating the integral scale and intensity of an atmospheric turbulence vertical velocity record assumed to be governed by the von Kármán transverse spectrum.

## Introduction

THE concern here is a single component (longitudinal, lateral, or vertical) of the turbulence velocity vector,<sup>1,3</sup> which will be assumed to have been drawn from an ergodic ensemble<sup>4</sup> of such records. The ensemble of velocity records is also assumed to have zero mean value and to be Gaussian.<sup>5</sup> Thus, all joint velocity statistics are assumed to be governed by the multidimensional normal distribution,<sup>4</sup> and the process is completely statistically characterized by its autocorrelation function or power spectral density,<sup>4</sup> which constitute a Fourier transform pair. von Kármán has postulated a mathematical form<sup>6,7</sup> for the three-dimensional velocity spectrum of turbulence that is in agreement with known required behavior<sup>8,9</sup> as a function of wave number, both at very small wave numbers and at larger wave numbers in the inertial subrange governed by the  $-5/3$  decay law. The transverse and longitudinal one-dimensional spectrum counterparts to the von Kármán three-dimensional spectrum each is a function of only two parameters, an integral scale  $L$  and an intensity  $\sigma$ . Thus, if the appropriate one of these one-dimensional spectrum mathematical forms is assumed to describe the power spectral density of a measured turbulence velocity record, as is commonplace,<sup>2,3,10</sup> then the implicitly postulated underlying random process of one-dimensional turbulence records is completely characterized by only two parameters,  $L$  and  $\sigma$ .

The problem addressed in this paper is how to best estimate the two parameters  $L$  and  $\sigma$  from a measured turbulence velocity record of finite duration that is assumed to have been drawn from an ergodic, Gaussian random process with zero mean value governed by either the von Kármán transverse or longitudinal power spectral form, as appropriate. The problem is formulated in a somewhat more general manner than this so as to include other two- and three-parameter spectral forms such as the Dryden two-parameter and Bullen three-parameter models.<sup>11</sup> Our approach is to treat the problem as a problem of parameter estimation in statistics.<sup>12</sup> Several ad hoc methods for estimating values of the integral scale are described on pp. 356-360 of Ref. 10.

## Evaluation of Scale and Intensity

### as a Statistical Problem of Parameter Estimation

In our conceptual turbulence model, an infinite ensemble of statistically stationary turbulence records of infinite duration is assumed to exist, where each record in the ensemble is governed by the same one-dimensional von Kármán spectrum possessing the same unknown integral scale  $L$  and intensity  $\sigma$ . A segment of duration  $T$  is isolated from one member of this ensemble and estimates of  $L$  and  $\sigma$  are computed. The method or rule by which  $L$  and  $\sigma$  are computed is called an *estimator*<sup>12</sup> and the values of  $L$  and  $\sigma$  computed are called *estimates*.<sup>12</sup>

If the above procedure were to be repeated with a different record of the same duration  $T$  drawn from the same ensemble, and values of  $L$  and  $\sigma$  were computed from this new record using the same method as used for the first record, generally different estimates of  $L$  and  $\sigma$  would be obtained—although these estimates might be quite close to those computed from the first record. Thus, if the above procedure were to be repeated an arbitrarily large number of times, each time using a different ensemble member of duration  $T$ , an empirically generated bivariate probability density function or histogram<sup>13</sup> of estimates of the two random variables  $L$  and  $\sigma$  would be generated. Some methods (estimators) of computing estimates of  $L$  and  $\sigma$  are clearly better than others.

### Properties of Estimators

Properties<sup>12,14</sup> of estimators particularly relevant to the present application are now described. Since in practice only a single turbulence record of duration  $T$  generally will be available, it is desirable that as  $T$  increases indefinitely estimates of  $L$  and  $\sigma$  computed from this record approach the true values  $L_0, \sigma_0$  of these parameters, defined by the infinite ensemble of records. An estimator possessing this property is said to be *consistent*.

It also is desirable that an estimator be unbiased. If, as described above, a family of estimates of  $L$  and  $\sigma$  is computed—each estimate of  $L, \sigma$  coming from a different turbulence record of the same finite duration  $T$ —and if the estimates of both  $L$  and  $\sigma$  thus obtained are averaged, then the estimator is said to be *unbiased* if the average values of  $L$  and  $\sigma$  approach the true values  $L_0$  and  $\sigma_0$  as the number of turbulence records used to compute the averages increases without limit. The property of an estimator being unbiased differs from the property of consistency in that an increasing number of records of fixed, finite duration  $T$  is dealt with in considering the question of bias, whereas a single record of

Received Nov. 1, 1982; revision received March 16, 1983. Copyright © 1982 by William D. Mark. Published by the American Institute of Aeronautics and Astronautics with permission.

\*Principal Scientist.

increasing length  $T$  is dealt with in considering the property of consistency.

Later in this paper, we shall see that instead of estimating  $L$  and  $\sigma$  it is more convenient to estimate  $\sigma^2 L$  and  $L$ . Our estimate of the square of the intensity is then computed from these estimates by  $\sigma^2 = (\sigma^2 L)/L$ . The intensity estimate  $\sigma$  is computed by taking the square root of  $\sigma^2$ . Alternatively, if the same general method of estimation were used to compute  $L$  and  $\sigma^2$  or  $L$  and  $\sigma$  directly from the same record and if the same values  $L$  and  $\sigma$  were obtained from each of the computations, then the method is said to be *invariant* under transformation of the parameters.<sup>14</sup>

If two different methods are used to generate two different histograms of a parameter from the same data, each histogram by one of the methods, the better method will yield the histogram more concentrated near the true value of the parameter. If both methods yield unbiased estimates, the better method will usually be the one yielding the smaller variance of the estimates. In comparing two unbiased estimators, the one yielding the smaller variance of the estimates is said to be *more efficient* than the other. An unbiased estimator yielding a variance as small or smaller than any other estimator is said to be an *efficient* estimator. The Cramér-Rao bound<sup>12,14,15</sup> yields the minimum variance that can be achieved by any estimator of a parameter from a given size of sample.

Properties of estimators that apply to large sample sizes—which correspond in the present application to large durations  $T$  of turbulence velocity records—are referred to as *asymptotic properties*. Maximum likelihood estimators of single or multiple<sup>12,16</sup> parameters are consistent, invariant, asymptotically unbiased, and asymptotically efficient. The variance of a maximum likelihood estimator asymptotically approaches the minimum variance given by the Cramér-Rao bound.<sup>12,14,15</sup> Multiple-parameter estimation by the maximum likelihood method asymptotically minimizes the generalized variance of the estimates.<sup>12</sup>

#### Maximum Likelihood Estimation of the Parameter in a Probability Density Function

The methodology developed in the present paper is based on the method of maximum likelihood originally introduced by Gauss. The method is generally treated<sup>12-16</sup> in the context of estimating one or more parameters—e.g., the mean and/or variance—of a probability density function of known functional form such as the normal probability density, which is completely described by its mean and variance. An estimate of such parameters is made from a random sample drawn from a population governed by the probability density under consideration. Let  $p(x;\theta)$  be the probability density of a random variable  $x$ , where  $\theta$  is an unknown parameter of the density function, such as its mean value. Let  $X_1, X_2, \dots, X_N$  be  $N$  samples drawn from a population whose probability density is  $p(x;\theta)$ . The basic idea of the maximum likelihood method is that the best choice of the unknown parameter  $\theta$  is the value that maximizes the probability of the sample  $X_1, X_2, \dots, X_N$  which has been drawn from the population that  $p(x;\theta)$  describes. The joint probability density of the randomly drawn sample  $X_1, X_2, \dots, X_N$  is

$$L(X_1, X_2, \dots, X_N; \theta) = \prod_{j=1}^N p(X_j; \theta) \quad (1)$$

which, when evaluated at the sample value  $X_1, X_2, \dots, X_N$ , is a function of the unknown parameter  $\theta$ . The function  $L(X_1, X_2, \dots, X_N; \theta)$ , defined by the right-hand side of Eq. (1), is called the likelihood function of the parameter  $\theta$ . Thus, the likelihood function is the joint probability density function of the sample, containing one or more unknown parameters  $\theta$  evaluated at the value of the sample.

Instead of finding the maximum value of the likelihood function directly, it usually is more convenient to determine  $\theta$

by maximizing the natural logarithm of the likelihood function, i.e., by finding the solution  $\theta$  of

$$\frac{d}{d\theta} \ln [L(X_1, X_2, \dots, X_N; \theta)] = 0 \quad (2)$$

Equation (2) is referred to as the likelihood equation for the parameter  $\theta$ . When Eq. (2) has more than one solution, the maximum likelihood solution is the value of  $\theta$  that maximizes Eq. (1). When the likelihood function contains more than one unknown parameter, Eq. (2) is replaced by a set of simultaneous equations, each being the partial derivative of the log likelihood function with respect to one of the parameters set equal to zero.

#### Joint Probability Density Function of Unsmoothed Turbulence Spectra

In the present application of the method of maximum likelihood, the integral scale and intensity of our turbulence ensemble will be estimated from the joint probability density function of the unsmoothed spectrum or periodogram<sup>4</sup>  $S(f)$  of a segment of duration  $T$  of a turbulence velocity record  $w(t)$ ,  $(-T/2) < t < (T/2)$ ,

$$S(f) \triangleq \frac{1}{T} \left| \int_{-T/2}^{T/2} w(t) \exp(-i2\pi ft) dt \right|^2 \quad (3)$$

The periodogram values to be utilized are the values  $S(f_j)$  at the set of discrete equispaced frequencies  $f_1, f_2, \dots$  where

$$f_j \triangleq j/T, \quad j=0, 1, 2, \dots \quad (4)$$

We shall consider values of  $S(f_j)$  only up to a finite value of  $f_j$ , say  $f_N = N/T$ ; hence, we require the joint probability density function  $p(S_1, S_2, \dots, S_N)$  of the periodogram values

$$S_j \triangleq S(f_j), \quad j=1, 2, \dots, N \quad (5)$$

considered as a function of the integral scale  $L$  and intensity  $\sigma$  of the turbulence ensemble.

The values of  $S(f)$  at the frequencies  $f_0, f_1, f_2, \dots$  are readily determined using the Fourier series representation of  $w(t)$  over the interval  $(-T/2) < t < (T/2)$ ,

$$w(t) = \sum_{n=-\infty}^{\infty} c_n \exp(i2\pi nt/T), \quad (-T/2) < t < (T/2) \quad (6)$$

where

$$c_n = \frac{1}{T} \int_{-T/2}^{T/2} w(t) \exp(-i2\pi nt/T) dt, \quad n=0, \pm 1, \pm 2, \dots \quad (7a)$$

$$= a_n - ib_n, \quad n=0, \pm 1, \pm 2, \dots \quad (7b)$$

are the Fourier series expansion coefficients,  $a_n$  and  $b_n$  both being real. Comparing Eqs. (3) and (7), we see that at frequencies  $f_n = n/T$ ,  $n=0, \pm 1, \pm 2, \dots$  the periodogram can be expressed in terms of the Fourier series expansion coefficients by

$$S(f_n) = T |c_n|^2 = T [a_n^2 + b_n^2], \quad n=0, \pm 1, \pm 2, \dots \quad (8)$$

Values of  $S(f)$  at intermediate values of  $f$  could be computed from the above values of  $c_n$  using the sampling theorem in the frequency domain.<sup>17</sup> Finally, we note that  $S(f)$  is an even function of  $f$ ; hence, it is completely determined by its values in the domain  $f \geq 0$  only.

In the present application, the utility of the joint probability density  $p(S_1, S_2, \dots, S_N)$  of periodogram random variables  $S_1, S_2, \dots, S_N$  arises from the fact that these random variables are approximately mutually statistically independent and that each  $S_j, j=1, 2, \dots, N$  is governed approximately by a probability density function of simple known functional form, i.e., the exponential density,

$$p(S_j) = \lambda_j \exp(-\lambda_j S_j), \quad S_j \geq 0, \quad j=1, 2, \dots, N$$

$$= 0, \quad S_j < 0, \quad j=1, 2, \dots, N \quad (9)$$

The approximate statistical independence of the periodogram samples  $S_1, S_2, \dots, S_N$  is proved in Appendix A along with the fact that each  $S_j$  is governed approximately by the exponential density function [Eq. (9)]. It follows that the approximate joint probability density  $p(S_1, S_2, \dots, S_N)$  of the periodogram samples  $S_1, S_2, \dots, S_N$  is expressed as the product of the individual density functions given by Eq. (9),

$$p(S_1, S_2, \dots, S_N) = \prod_{j=1}^N \lambda_j \exp(-\lambda_j S_j), \quad S_j \geq 0, \quad j=1, 2, \dots, N$$

$$= 0, \quad S_j < 0, \quad j=1, 2, \dots, N \quad (10)$$

It is shown in Appendix A that the above-mentioned approximations pertaining to the statistical independence and probability density functions of  $S_j, j=1, 2, \dots, N$  approach exact results as the duration  $T$  of the turbulence sample becomes arbitrarily large relative to the integral scale of the turbulence.

For  $j=1, 2, \dots, N$  it is easily shown from Eq. (9) that  $\lambda_j$  is the reciprocal of the expected value of  $S_j$ , i.e.,

$$\lambda_j = 1/E\{S_j\}, \quad j=1, 2, \dots, N \quad (11)$$

where  $E\{\dots\}$  denotes the mathematical expectation operation.<sup>4,13-15</sup> It is this relationship that will permit us to express the joint density [Eq. (10)] in terms of the integral scale and the intensity of the turbulence.

### Likelihood Equations for a General Class of Turbulence Spectra

Introducing the notation

$$\bar{S}_j \equiv E\{S_j\} = 1/\lambda_j, \quad j=1, 2, \dots, N \quad (12)$$

we see that the logarithm to the base  $e$  of Eq. (10) can be expressed as

$$\ln[p(S_1, S_2, \dots, S_N)] = [\ln(\lambda_1 \lambda_2 \dots \lambda_N)]$$

$$- [\lambda_1 S_1 + \lambda_2 S_2 + \dots + \lambda_N S_N] = - \left\{ [\ln(\bar{S}_1 \bar{S}_2 \dots \bar{S}_N)] \right.$$

$$\left. + \left[ \frac{S_1}{\bar{S}_1} + \frac{S_2}{\bar{S}_2} + \dots + \frac{S_N}{\bar{S}_N} \right] \right\} \quad (13)$$

where, for brevity, we have left out the statement that the right-hand side is valid only for  $S_j \geq 0, j=1, 2, \dots, N$ . Let us now introduce a general class of two-parameter spectrum functional forms that includes the von Kármán and Dryden transverse and longitudinal spectra<sup>11</sup> as special cases,

$$E\{S_j\} = \bar{S}_j = \sigma^2 L F_j(L), \quad j=1, 2, \dots, N \quad (14)$$

where, for a given frequency index  $j$ ,  $F_j(L)$  is a function of the integral scale  $L$  but is independent of  $\sigma$ . Substituting Eq. (14) into Eq. (13) yields

$$\ln[p(S_1, S_2, \dots, S_N)] = - \left\{ N \ln(\sigma^2 L) + \ln F_1(L) \right.$$

$$+ \ln F_2(L) + \dots + \ln F_N(L) + \frac{1}{\sigma^2 L} \left[ \frac{S_1}{F_1(L)} \right.$$

$$\left. + \frac{S_2}{F_2(L)} + \dots + \frac{S_N}{F_N(L)} \right] \left. \right\} \quad (15)$$

Equation (15) evaluated at the periodogram sample  $S_1, S_2, \dots, S_N$  and considered as a function of the two spectrum parameters  $L$  and  $\sigma$  is the logarithm of the likelihood function of  $L$  and  $\sigma$ .

The values of  $L$  and  $\sigma$  that maximize Eq. (15) for a given periodogram sample  $S_1, S_2, \dots, S_N$  are the maximum likelihood values of  $L$  and  $\sigma$ . However, from the functional form of the right-hand side of Eq. (15), we see that it is more convenient to treat the right-hand side of Eq. (15) as a function of the two parameters  $(\sigma^2 L)$  and  $L$  rather than  $\sigma$  and  $L$ . The invariance property of maximum likelihood estimators guarantees that maximum likelihood solutions for  $\sigma^2 L$  and  $L$  will yield the same values of  $\sigma$  and  $L$  that direct maximum likelihood equations for  $\sigma$  and  $L$  would yield. To find the equations that yield maximum likelihood estimates of  $\sigma^2 L$  and  $L$ , we differentiate Eq. (15) with respect to  $\sigma^2 L$  and  $L$  and set the resulting expressions equal to zero,

$$\frac{\partial \ln[p(S_1, S_2, \dots, S_N; \sigma^2 L, L)]}{\partial(\sigma^2 L)} = \frac{1}{(\sigma^2 L)^2} \sum_{j=1}^N \left[ \frac{S_j}{F_j(L)} - \sigma^2 L \right] \quad (16)$$

and

$$\frac{\partial \ln[p(S_1, S_2, \dots, S_N; \sigma^2 L, L)]}{\partial L}$$

$$= \frac{1}{\sigma^2 L} \sum_{j=1}^N \left[ \frac{d}{dL} \ln F_j(L) \right] \left[ \frac{S_j}{F_j(L)} - \sigma^2 L \right] \quad (17)$$

where the parametric dependence of  $p(S_1, S_2, \dots, S_N)$  on  $\sigma^2 L$  and  $L$  has been indicated in the arguments in the left-hand sides of Eqs. (16) and (17) for clarity. Setting Eq. (16) equal to zero yields our likelihood equation for  $\sigma^2 L$ ,

$$\sigma^2 L = \frac{1}{N} \sum_{j=1}^N \frac{S_j}{F_j(L)} \quad (18)$$

and setting Eq. (17) equal to zero yields our likelihood equation for  $L$  after substitution of Eq. (18),

$$\sum_{j=1}^N \left[ \frac{d}{dL} \ln F_j(L) \right] \left[ \frac{S_j}{F_j(L)} - \frac{1}{N} \sum_{i=1}^N \frac{S_i}{F_i(L)} \right] = 0 \quad (19)$$

### Specialization to von Kármán Spectra

To specialize Eqs. (18) and (19) to the von Kármán transverse and longitudinal spectral forms,<sup>11</sup> we require the functions  $F_j(L)$  defined by Eq. (14) and the derivatives of their natural logarithms with respect to  $L$ ,

$$G_j(L) \triangleq \frac{d}{dL} \ln F_j(L) \quad (20)$$

For the von Kármán transverse spectrum, we have

$$F_j(L) \equiv F(k_j; L) = \frac{1 + 188.75 L^2 k_j^2}{(1 + 70.78 L^2 k_j^2)^{11/6}} \quad (21)$$

$$G_j(L) \equiv \frac{d}{dL} \ln F(k_j; L) = \frac{1}{L} \frac{117.97 L^2 k_j^2 (1 - 188.75 L^2 k_j^2)}{(1 + 70.78 L^2 k_j^2) (1 + 188.75 L^2 k_j^2)} \quad (22)$$

For the von Kármán longitudinal spectrum, we have

$$F_j(L) \equiv F(k_j; L) = \frac{2}{(1 + 70.78L^2k_j^2)^{5/6}} \quad (23)$$

$$G_j(L) \equiv \frac{d}{dL} \ln F(k_j; L) = -\frac{1}{L} \frac{117.97L^2k_j^2}{1 + 70.78L^2k_j^2} \quad (24)$$

The exact values of the constants in Eqs. (21-24) are the left-hand sides of

$$25\pi [\Gamma(4/3)/\Gamma(11/6)]^2 = 70.78 \quad (25)$$

$$(200/3)\pi [\Gamma(4/3)/\Gamma(11/6)]^2 = 188.75 \quad (26)$$

$$(125/3)\pi [\Gamma(4/3)/\Gamma(11/6)]^2 = 117.97 \quad (27)$$

where  $\Gamma(\cdot)$  is the gamma function. The spectra defined by Eqs. (14), (21), and (23) are two-sided spectra satisfying

$$\sigma^2 = \int_{-\infty}^{\infty} \sigma^2 L F(k; L) dk \quad (28)$$

where  $k$  is the wave number in cycles/unit distance and  $L$  the integral scale of the longitudinal spectrum, which is twice the integral scale of the transverse spectrum.<sup>2,11</sup>

Equations (18) and (19) are a pair of likelihood equations for  $\sigma^2 L$  and  $L$  that involve the periodogram values  $S_j$ ,  $j=1, 2, \dots, N$  as parameters. This pair of equations is applicable to both the von Kármán transverse and longitudinal spectral forms when the functions defined by Eqs. (20-24) are utilized in them, as appropriate. Equation (19) involves only one unknown,  $L$ , and therefore may be solved first. Once  $L$  is obtained from Eq. (19), Eq. (18) may be solved for  $\sigma$ . If we consider our turbulence sample  $w(t)$  to be a function of time of duration  $T$ , then the values of  $S_j$  to be used in Eqs. (18) and (19) are those obtained from Eq. (3) at the values of  $f=j/T$ ,

$$S_j = \frac{1}{T} \left| \int_{-T/2}^{T/2} w(t) \exp(-i2\pi j t/T) dt \right|^2, \quad j=1, 2, \dots, N \quad (29)$$

The corresponding wave number values  $k_j$  to be used in Eqs. (20-24), as appropriate, are obtained from Taylor's hypothesis,  $k=f/V$ , which when combined with Eq. (4) yields

$$k_j = j/(VT) \quad (30)$$

where  $V$  is the speed of the probe or measuring aircraft relative to the mean speed of the turbulence medium. The frequencies  $f_j=j/T$  at which the periodogram samples  $S_j$  defined by Eq. (29) are required are precisely those values provided by the discrete Fourier transform of a waveform of duration  $T$ , which is usually implemented by the fast Fourier transform algorithm. Further discussion of the likelihood equations (18) and (19) is contained in Ref. 18. Discussion of a general method similar to that contained herein can be found in Ref. 19.

Likelihood equations for the three-parameter Bullen transverse and longitudinal spectra<sup>11</sup> are derived in Appendix B. The Dryden spectrum<sup>11</sup> counterparts to Eqs. (21-24) are obtained from Eqs. (B8), (B9), (B11), and (B12) with the aid of Eq. (B14) by setting  $n=1/2$  in these equations.

#### Coefficients of Variation of Maximum Likelihood Estimates of von Kármán Spectrum Parameters

Since the periodogram sample  $S_1, S_2, \dots, S_N$  is an  $N$ -dimensional random variable, estimates of  $L$  and  $\sigma^2$  computed from  $S_1, S_2, \dots, S_N$  or from the original turbulence sample function  $w(t)$  are also random variables. In an analysis<sup>18</sup> too long to be included here, we have shown that

the large  $T$ /large  $N$  asymptotic expressions for the coefficients of variation<sup>15</sup>  $\sigma_L/L$  and  $\sigma_{\sigma^2}/\sigma^2$  of the maximum likelihood estimates  $\hat{L}$  and  $\hat{\sigma}^2$  of  $L$  and  $\sigma^2$ , respectively, are,

for the von Kármán transverse spectrum

$$\sigma_L/L = 1.50(L/\mathcal{L})^{1/2}, \quad \sigma_{\sigma^2}/\sigma^2 = 1.0008(L/\mathcal{L})^{1/2} \quad (31)$$

for the von Kármán longitudinal spectrum

$$\sigma_L/L = 1.96(L/\mathcal{L})^{1/2}, \quad \sigma_{\sigma^2}/\sigma^2 = 1.3092(L/\mathcal{L})^{1/2} \quad (32)$$

where  $L$  and  $\sigma^2$  denote, respectively, the true integral scale and true mean square value of the process, and  $\mathcal{L}$  denotes the length of the stationary record from which the maximum likelihood estimates of  $L$  and  $\sigma^2$  are computed.  $L$  and  $\mathcal{L}$  must, of course, be measured in the same units of length. Equations (31) and (32) describe typical fractional errors in maximum likelihood estimates of  $L$  and  $\sigma^2$  obtained using Eqs. (18) and (19). Since maximum likelihood estimators are asymptotically efficient, it would seem that the above coefficients of variation are the smallest values achievable for stationary Gaussian turbulence records governed by von Kármán transverse or longitudinal spectra.

#### Application

The method described herein for estimating  $L$  and  $\sigma$  has been applied to the 19 min vertical record shown in Fig. 1.<sup>20</sup> First, the (smoothed) power spectral density of this record was computed using the Papoulis window function<sup>21</sup> and the method described in Appendix B of Ref. 22 (using  $M=6590.5$  m, which corresponded to 1024 temporal sample points of the digitized record). Before computing the power spectral density of the record, its mean value was computed and removed. The power spectral density obtained from this computation is shown by the discrete points in Fig. 2.

The solid curve shown in Fig. 2 is the von Kármán transverse power spectral density,

$$\Phi(k) = \sigma^2 L \frac{1 + 188.75L^2k^2}{(1 + 70.78L^2k^2)^{11/6}} \quad (33)$$

according to Eqs. (14) and (21). The values of  $L$  and  $\sigma^2$  used in plotting Eq. (33) in Fig. 2 are

$$L = 309.4 \text{ m}, \quad \sigma^2 = 1.326 \text{ (m/s)}^2 \quad (34)$$

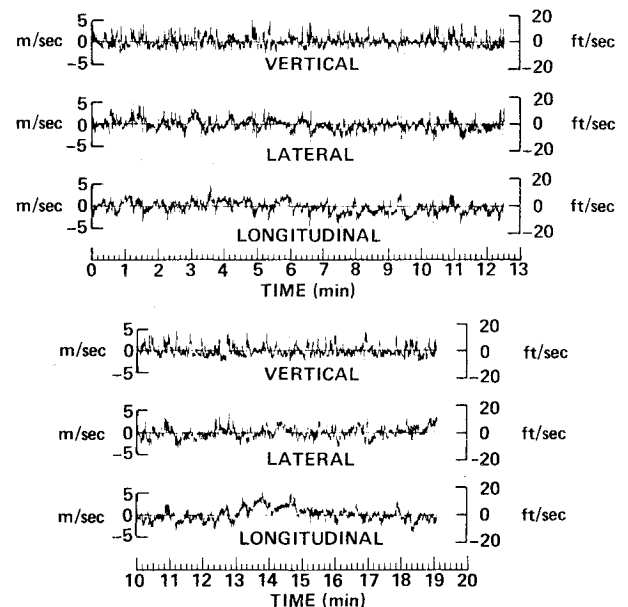


Fig. 1 Low-altitude turbulence records: convective conditions, aircraft speed 129 m/s (422 ft/s) (from Ref. 20, Fig. 4, p. 282).

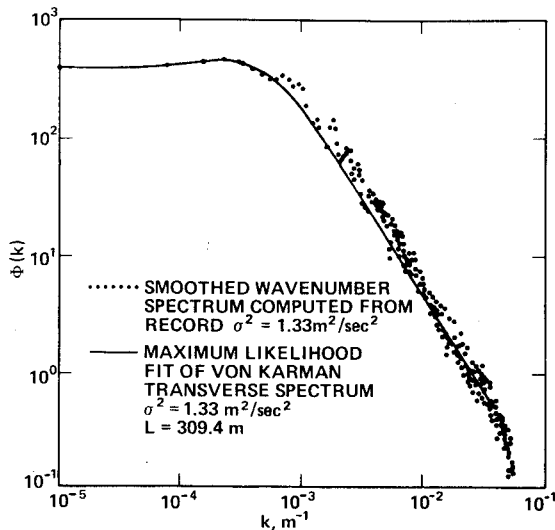


Fig. 2 Comparison of smoothed wave number spectrum computed from vertical record shown in Fig. 1 and maximum likelihood fit of von Kármán transverse spectrum.

The value of  $L$  was computed from the periodogram sample values  $S_j$  of Eq. (29) using Eq. (19). The value of  $\sigma^2$  was then computed by Eq. (18) using this value of  $L$ . The functions  $F_j(L)$  and  $(d/dL)\ln F_j(L)$  used in Eqs. (18) and (19) were those given by Eqs. (21) and (22). Good agreement is shown in Fig. 2 between the discrete points and the von Kármán transverse spectrum determined by Eqs. (33) and (34).

Equation (19) expresses  $L$  as an implicit function of the periodogram values  $S_j$ . The value of  $L = 309.4$  m was computed in the following manner. From Eqs. (19) and (20), we see that for a given periodogram sample  $S_1, S_2, \dots, S_N$  the value of  $L$  that sets the error

$$E(L) \triangleq \frac{1}{N} \sum_{j=1}^N G_j(L) \left\{ \left[ \frac{1}{N} \sum_{i=1}^N \frac{S_i}{F_i(L)} \right] - \frac{S_j}{F_j(L)} \right\} \quad (35)$$

equal to zero is a solution to Eq. (19). The correct value of  $L = 309.4$  m was determined by the combined trial-and-error/linear interpolation technique illustrated in Fig. 3, where the encircled numbers designate the sequential order that the values of  $E(L)$  were computed by Eq. (35). The first trial value of  $L = 305$  m (1000 ft) was chosen arbitrarily. This value of  $L$  yielded a negative value of  $E(L)$ , indicating that a larger value of  $L$  was required. The second trial value of  $L = 335.5$  m (1100 ft) was then chosen, yielding a positive value of  $E(L)$  as indicated by the point labeled by the encircled 2 in Fig. 3. Linear interpolation between the first and second trial points yielded the third trial value of  $L$ , which in turn yielded the third value of  $E(L)$  by Eq. (35) that was slightly too large, as Fig. 3 shows. Thus, a smaller fourth trial value of  $L$  was chosen, which was 3.05 m (10 ft) smaller than the third trial value of  $L$ . Linear interpolation between the values of  $E(L)$  computed from the third and fourth trial values of  $L$  yielded the fifth and final value of  $L = 309.4$  m shown in Fig. 3.

An estimate of  $\sigma^2$  was also computed by the more conventional method of squaring and averaging the sample points of the vertical record shown in Fig. 1. The computed mean square value was

$$\sigma^2 = 1.331 \text{ (m/s)}^2 \quad (36)$$

Although the maximum likelihood method used to compute the value of  $\sigma^2$  given by Eq. (34) is not the same as the squaring and averaging procedure used to compute the value of  $\sigma^2$  given by Eq. (36), the two values agree, quite remarkably, when rounded to three significant figures. Since the assumption of a von Kármán transverse spectrum—with the value of  $L = 309.4$  m—was used in the computation of  $\sigma^2$  given by Eq. (34), the close agreement of the two values of  $\sigma^2$

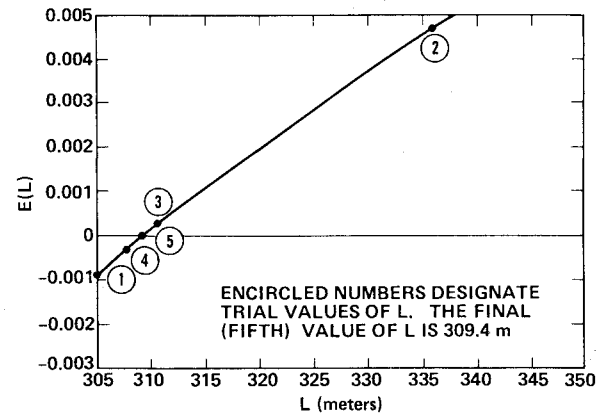


Fig. 3 Combined trial-and-error/interpolation solution for integral scale  $L$  of vertical record shown in Fig. 1.

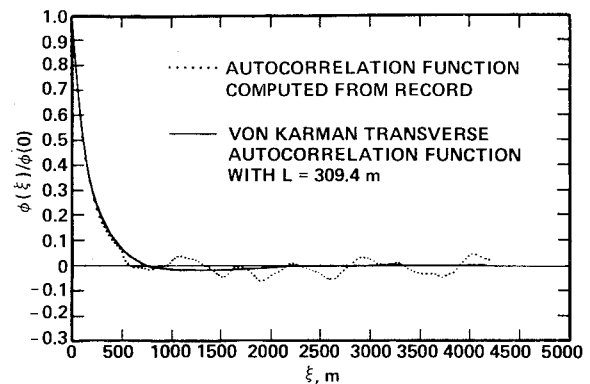


Fig. 4 Comparison of autocorrelation function computed from vertical record shown in Fig. 1 and von Kármán transverse autocorrelation function with integral scale  $L$  computed as in Fig. 3.

given by Eqs. (34) and (36) provides verification of the excellent representation of the empirical spectrum provided by the von Kármán transverse spectrum [Eq. (33)] with  $L = 309.4$  m.

The autocorrelation function of the vertical record shown in Fig. 1 is compared in Fig. 4 with the von Kármán transverse autocorrelation function,

$$\phi(\xi) \triangleq \sigma^2 \frac{2^{2/3}}{\Gamma(1/3)} \left( \frac{\beta \xi}{L} \right)^{1/3} \left[ K_{1/3} \left( \frac{\beta \xi}{L} \right) - \frac{\beta \xi}{2L} K_{5/3} \left( \frac{\beta \xi}{L} \right) \right] \quad (37)$$

where

$$\beta \triangleq \frac{\sqrt{\pi} \Gamma(5/6)}{\Gamma(1/3)} \quad (38)$$

and  $L$  is the integral scale given by Eq. (34), the  $K_n(\cdot)$  are modified Bessel functions of the second kind of order  $n$ , and  $\Gamma(\cdot)$  is the gamma function. The empirical autocorrelation function in Fig. 4 was computed by the method described in Appendix B of Ref. 22.

Substituting  $L = 129 \times 19 \times 60 = 147,060$  m and  $L = 309.4$  m [from Fig. 1 and Eqs. (34), respectively] into Eq. (31), we find

$$\sigma_L/L = 0.069 \approx 7\%, \quad \sigma_{\sigma^2}/\sigma^2 = 0.046 \approx 5\% \quad (39)$$

which represent the approximate fractional errors to be expected in the estimates of  $L$  and  $\sigma^2$  given by Eq. (34). The records shown in Fig. 1 are unusually long and well behaved. Often, estimates of  $L$  and  $\sigma^2$  must be made from much shorter whole records or record segments, which will result in significantly larger uncertainties in such estimates according to Eqs. (31) and (32). Various ad hoc estimation methods<sup>10</sup> of the integral scale will result in still larger uncertainties.

### Discussion

In Appendix D of Ref. 22, we have shown that the large  $T$  asymptotic expressions for the coefficients of variation<sup>15</sup>  $\sigma_{\hat{\sigma}^2}/\sigma^2$  of estimates  $\hat{\sigma}^2$  of  $\sigma^2$  obtained by the conventional method of squaring and averaging a record of length  $\mathcal{L}$  are,

for the von Kármán transverse spectrum

$$\sigma_{\hat{\sigma}^2}/\sigma^2 = 1.0339(L/\mathcal{L})^{1/2} \quad (40)$$

for the von Kármán longitudinal spectrum

$$\sigma_{\hat{\sigma}^2}/\sigma^2 = 1.3161(L/\mathcal{L})^{1/2} \quad (41)$$

which are only negligibly larger than their maximum likelihood counterparts given in Eqs. (31) and (32), respectively. Thus, the a priori information of the functional form of the spectrum given by Eqs. (21) or (23), as appropriate, that is used in the likelihood equation (18) for estimation of  $\sigma^2$  provides no practical advantage over the more conventional squaring and averaging estimation procedure. Since this latter procedure requires no a priori information about the functional form of the spectrum, it is probably the more reliable method.

The situation with regard to estimation of  $L$  is fundamentally different. From the fact that the two-sided power spectral density  $S_\ell(k)$  of a record is the Fourier transform of the autocorrelation function  $\phi_\ell(\xi)$  of the record [e.g., Ref. 4, pp. 101-103], we have

$$\begin{aligned} S_\ell(0) &= \int_{-\infty}^{\infty} \phi_\ell(\xi) d\xi = 2 \int_0^{\infty} \phi_\ell(\xi) d\xi \\ &= 2\sigma^2 \int_0^{\infty} [\phi_\ell(\xi)/\phi_\ell(0)] d\xi = 2\sigma^2 L \end{aligned} \quad (42)$$

hence,

$$L = (1/2\sigma^2) S_\ell(0) \quad (43)$$

where subscript  $\ell$  denotes that the definition of  $L$  given in Eq. (42) applies to the longitudinal turbulence component.<sup>2,11</sup> Since from Eqs. (7a) and (7b) we have  $b_0 = 0$ , it follows from Eq. (8) that periodogram estimates  $S(0)$  of  $S_\ell(0)$  are governed by a gamma probability density function with  $n=1$  statistical degrees of freedom, which has a coefficient of variation of  $\sqrt{2}$  (Ref. 23, p. 415). Thus, if  $L$  is estimated using Eq. (43) from the periodogram value  $S(0)$  given by Eq. (8), it follows that the coefficient of variation of such an estimate  $\hat{L} = S(0)/2\sigma^2$  will asymptotically approach  $\sqrt{2}$  as the record length becomes arbitrarily large. [Also see Eq. (A14) for  $n=0$ .]

The statistical reliability of this inherently poor estimation procedure can be substantially improved by utilizing several additional periodogram sample values  $S_1, S_2, \dots, S_B$ ,  $B \propto (\mathcal{L}/L)$  in the neighborhood of the periodogram origin  $k=0$ , but such an approach requires an a priori assumption about the behavior of the functional form of the spectrum—e.g.,  $F_\ell(L)=1$  or 2 as appropriate—in a finite neighborhood of  $k$  about  $k=0$ . [This procedure is essentially equivalent to using Eq. (18) with  $N=B$  to solve for  $L$  with  $\sigma^2$  estimated by the conventional method.] The maximum likelihood method leading to Eq. (19) for  $L$  utilizes in an optimum manner an arbitrarily large number  $N$  of periodogram sample values  $S_1, S_2, \dots, S_N$ , and the a priori functional form of the entire spectrum  $F_\ell(L)$  given by Eq. (21) or (23), as appropriate. The coefficients of variation  $\sigma_{\hat{L}}/L$  of such maximum likelihood estimates of  $L$  given in Eqs. (31) and (32) tend to zero as  $\mathcal{L}$  becomes arbitrarily large, in contrast to the asymptotic limit of  $\sqrt{2}$  cited above. Estimation procedures for atmospheric turbulence records<sup>20</sup> not well represented by von Kármán spectra are developed in Ref. 18.

### Appendix A: Statistical Independence and Probability Density Functions of Periodogram Samples

To consider the statistical properties of the periodogram samples  $S_j = S(f_j)$ ,  $j=1, 2, \dots, N$  generated from a single record  $w(t)$  of duration  $T$ , we must utilize the entire conceptual ensemble of such records, where each record within this ensemble is obtained by isolating a segment of duration  $T$ , say  $(-T/2) < t < (T/2)$ , from the corresponding record in the original ensemble of ergodic records. Utilizing the Fourier series coefficients [Eq. (7)] of a typical ensemble member of this process of truncated records, consider

$$\begin{aligned} c_n c_m^* &= (a_n - ib_n)(a_m + ib_m) \\ &= (a_n a_m + b_n b_m) + i(a_n b_m - a_m b_n) \end{aligned} \quad (A1)$$

and

$$c_n c_m = (a_n a_m - b_n b_m) - i(a_n b_m + a_m b_n) \quad (A2)$$

where the superscript asterisk denotes the complex conjugate. Taking the expected values of Eqs. (A1) and (A2), we find that if

$$\text{Re}E\{c_n c_m^*\} = 0 \quad \text{and} \quad \text{Re}E\{c_n c_m\} = 0 \quad (A3)$$

then we must have

$$E\{a_n a_m\} = -E\{b_n b_m\} = E\{b_n b_m\} \equiv 0 \quad (A4)$$

whereas, if

$$\text{Im}E\{c_n c_m^*\} = 0 \quad \text{and} \quad \text{Im}E\{c_n c_m\} = 0 \quad (A5)$$

then we must have

$$E\{a_n b_m\} = E\{a_m b_n\} = -E\{a_m b_n\} \equiv 0 \quad (A6)$$

where Re and Im denote, respectively, the real and imaginary parts. Thus, satisfaction of all four conditions of Eqs. (A3) and (A5) for all integers  $m, n$  would guarantee that all pairs of coefficients  $a_m, a_n, b_m, b_n$  are uncorrelated.

From Eq. (7a), we have

$$\begin{aligned} E\{c_n c_m^*\} &= \frac{1}{T^2} \int_{-T/2}^{T/2} \int_{-T/2}^{T/2} E\{w(t_1) w(t_2)\} \\ &\quad \times \exp[-i2\pi(nt_1 - mt_2)/T] dt_1 dt_2 \\ &= \frac{1}{T^2} \int_{-T/2}^{T/2} \int_{-T/2}^{T/2} \phi_w(t_2 - t_1) \\ &\quad \times \exp[-i2\pi(nt_1 - mt_2)/T] dt_1 dt_2 \end{aligned} \quad (A7)$$

where  $\phi_w(t_2 - t_1)$  is the autocorrelation function of the original stationary turbulence process  $w(t)$ . Since truncation of the ensemble members outside of the interval  $(-T/2) < t < (T/2)$  has not affected their behavior within this interval,  $\phi_w(t_2 - t_1)$  is a function of  $t_2 - t_1$  when  $t_1$  and  $t_2$  both lie within  $(-T/2) < t < (T/2)$  as in Eq. (A7).

Defining<sup>17</sup>

$$\begin{aligned} \text{rect}(t) &\triangleq 1, \quad |t| < 1/2 \\ &\triangleq 0, \quad |t| > 1/2 \end{aligned} \quad (A8)$$

we can rewrite Eq. (A7) as

$$\begin{aligned} E\{c_n c_m^*\} &= \frac{1}{T^2} \int_{-\infty}^{\infty} \int_{-\infty}^{\infty} \text{rect}(t_1/T) \text{rect}(t_2/T) \\ &\quad \times \phi_w(t_2 - t_1) \exp[-i2\pi(nt_1 - mt_2)/T] dt_1 dt_2 \end{aligned} \quad (A9)$$

Let us introduce the new coordinates  $t, \tau$  defined by

$$t \triangleq \frac{t_1 + t_2}{2}, \quad \tau \triangleq t_2 - t_1 \quad (\text{A10})$$

hence,

$$t_1 = t - \tau/2, \quad t_2 = t + \tau/2 \quad (\text{A11})$$

Substituting Eqs. (A11) into Eq. (A9) and recognizing that  $|\partial(t, \tau)/\partial(t_1, t_2)| = 1$ , we have after minor rearrangement of the exponent

$$\begin{aligned} E\{c_n c_m^*\} &= \frac{1}{T^2} \int_{-\infty}^{\infty} \int_{-\infty}^{\infty} \text{rect}\left(\frac{t}{T} - \frac{\tau}{2T}\right) \text{rect}\left(\frac{t}{T} + \frac{\tau}{2T}\right) \\ &\quad \times \phi_w(\tau) \exp\left\{-i2\pi\left[(n-m)\frac{t}{T} - (n+m)\frac{\tau}{2T}\right]\right\} dt d\tau \\ &= \int_{-\infty}^{\infty} \left\{ \int_{-\infty}^{\infty} \text{rect}\left(t' - \frac{\tau'}{2}\right) \text{rect}\left(t' + \frac{\tau'}{2}\right) \right. \\ &\quad \times \exp[-i2\pi(n-m)t'] dt' \Big\} \phi_w(T\tau') \\ &\quad \times \exp[i2\pi(n+m)\tau'/2] d\tau' \end{aligned} \quad (\text{A12})$$

where we have introduced the dimensionless coordinates  $t' \triangleq t/T$  and  $\tau' \triangleq \tau/T$  in going to the second form of Eq. (A12). The inner integral in Eq. (A12) is the Fourier transform of the quantity  $\text{rect}[t' - (\tau'/2)]\text{rect}[t' + (\tau'/2)]$  considered as a function of  $t'$  with  $\tau'$  held constant. This function is illustrated in Fig. A1, where we see that for a given value of  $\tau'$  it is unity within the interval  $|t'| < (1 - |\tau'|)/2$  and zero outside this interval. Hence, again utilizing Eq. (A8), we see that the last form of Eq. (A12) is equivalent to

$$\begin{aligned} E\{c_n c_m^*\} &= \int_{-1}^1 \left\{ \int_{-\infty}^{\infty} \text{rect}\left(\frac{t'}{1 - |\tau'|}\right) \exp[-i2\pi(n-m)t'] dt' \right\} \\ &\quad \times \phi_w(T\tau') \exp[i2\pi(n+m)\tau'/2] d\tau' \\ &= \int_{-1}^1 (1 - |\tau'|) \frac{\sin[\pi(n-m)(1 - |\tau'|)]}{\pi(n-m)(1 - |\tau'|)} \phi_w(T\tau') \\ &\quad \times \cos[2\pi(n+m)\tau'/2] d\tau' \end{aligned} \quad (\text{A13})$$

where in going to the second expression in Eq. (A13) we have used a well-known result<sup>17</sup> for the Fourier transform of the rect function as described by the quantity within the braces in the first expression in Eq. (A13), and have replaced the second exponential function by a cosine function because the remainder of the integrand in the second expression in Eq. (A13) is an even function of  $\tau'$ . The original expression for  $E\{c_n c_m^*\}$  given by Eq. (A7) involves a double integration of a complex function, whereas the last form of Eq. (A13) expresses  $E\{c_n c_m^*\}$  as a single integration of a real function. For the case  $m=n$ , it follows directly from Eq. (A13) using  $\lim_{x \rightarrow 0} (\sin x/x) = 1$  that we have exactly

$$E\{|c_n|^2\} = \int_{-1}^1 (1 - |\tau'|) \phi_w(T\tau') \cos(2\pi n\tau') d\tau' \quad (\text{A14})$$

To examine the second condition in each of Eqs. (A3) and (A5), we note from Eq. (7a) that  $c_m = c_{-m}^*$ ; hence, from Eq. (A13), we have

$$\begin{aligned} E\{c_n c_m\} &= \int_{-1}^1 (1 - |\tau'|) \frac{\sin[\pi(n+m)(1 - |\tau'|)]}{\pi(n+m)(1 - |\tau'|)} \phi_w(T\tau') \\ &\quad \times \cos[2\pi(n-m)\tau'/2] d\tau' \end{aligned} \quad (\text{A15})$$

Since the right-hand sides of Eqs. (A13) and (A15) are both real, it follows that both of the conditions in Eq. (A5) are

satisfied exactly; hence, Eq. (A6) is also satisfied exactly, which states that pairs of the coefficients  $a_n$  and  $b_m$  are uncorrelated for all  $m, n$ .

We shall now show that for  $m \neq \pm n$  and sufficiently large values of  $T$  both conditions in Eq. (A3) are satisfied approximately, from which it follows that the condition of Eq. (A4) is also satisfied approximately for  $m \neq \pm n$ . To establish this result, let us first denote a typical correlation interval (e.g., the integral scale) associated with the autocorrelation function  $\phi_w(\tau)$  by  $\tau_L$ . Thus, for all delays  $|\tau|$  larger than a few times  $\tau_L$ , the value of  $\phi_w(\tau)$  is negligible. Let us now assume that  $T \gg \tau_L$ ; hence,

$$\tau'_L \triangleq \tau_L/T \ll 1 \quad (\text{A16})$$

When the condition in Eq. (A16) is satisfied,  $\phi_w(T\tau')$  is negligible for all  $\tau'$  except values in the immediate vicinity of  $\tau' = 0$ . However, it is directly apparent that

$$\lim_{\tau' \rightarrow 0} \frac{\sin[\pi(n \mp m)(1 - |\tau'|)]}{\pi(n \mp m)(1 - |\tau'|)} = 0, \quad m \neq \pm n \quad (\text{A17})$$

hence, when  $T \gg \tau_L$  as in Eq. (A16) it follows from Eq. (A17) that for  $m \neq \pm n$  the right-hand sides of Eqs. (A13) and (A15) are approximately zero. It then follows from Eqs. (A3) and (A4) that when  $T \gg \tau_L$ , we have

$$\begin{aligned} E\{a_n a_m\} &\approx 0 \quad \text{and} \quad E\{b_n b_m\} \approx 0 \\ m &\neq \pm n, \quad T \gg \tau_L \end{aligned} \quad (\text{A18})$$

In summary, we have shown that for all  $m, n$  the values of  $a_n$  and  $b_m$  are strictly uncorrelated, as indicated by Eq. (A6); whereas for  $m \neq \pm n$  and  $T \gg \tau_L$  the values of  $a_n$  and  $a_m$  are approximately uncorrelated, as are the values of  $b_n$  and  $b_m$  as indicated by Eq. (A18).<sup>4</sup>

Furthermore, for  $m=n$  we see from Eq. (A15) that

$$\begin{aligned} E\{c_n^2\} &= \int_{-1}^1 (1 - |\tau'|) \frac{\sin[2\pi n(1 - |\tau'|)]}{2\pi n(1 - |\tau'|)} \phi_w(T\tau') d\tau' \\ &= \int_{-1}^1 (1 - |\tau'|) \phi_w(T\tau') d\tau', \quad n=0 \\ &\approx 0, \quad n \neq 0, \quad T \gg \tau_L \end{aligned} \quad (\text{A19})$$

where the last line follows from Eq. (A17) whenever  $T \gg \tau_L$ . From Eq. (A2) and the second relation in Eq. (A5), it then

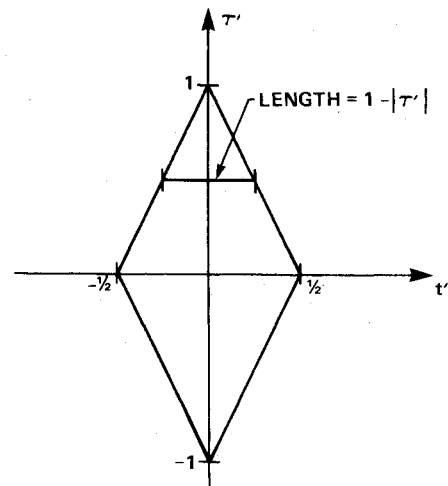


Fig. A1 Product  $\text{rect}[t' - (\tau'/2)]\text{rect}[t' + (\tau'/2)]$  is unity inside the diamond and zero outside of it.

follows from the last line in Eq. (A19) that

$$E\{a_n^2\} \approx E\{b_n^2\}, \quad n \neq 0, \quad T \gg \tau_L \quad (\text{A20})$$

Since the turbulence process  $w(t)$  has been assumed Gaussian and the transformation Eq. (7a) is linear, it follows<sup>4,15</sup> that  $c_n$ ,  $a_n$ , and  $b_n$ ,  $n=0,1,2,\dots$  are jointly distributed normal random variables. Furthermore, from Eq. (7b) we see that

$$|c_n|^2 = a_n^2 + b_n^2 \quad (\text{A21})$$

Since we have shown that values of  $a_n$  and  $b_n$  are strictly uncorrelated and normally distributed, it follows that  $a_n^2$  and  $b_n^2$  are independent random variables possessing approximately the same mean square value for  $n \neq 0$  according to Eq. (A20). Hence, for  $n=1,2,\dots$  we see from Eq. (A21) that  $|c_n|^2$  is the sum of the squares of two independent normally distributed random variables possessing approximately the same variance (and zero mean) from which it follows<sup>15,23</sup> that  $|c_n|^2$  is approximately exponentially distributed whenever  $T \gg \tau_L$ . Furthermore, from the joint normally distributed property of the  $a_n$  and  $b_m$ ,  $n,m=0,1,2,\dots$  and Eqs. (A6) and (A18), it follows that the random variables  $|c_n|^2$ ,  $n=0,1,2,\dots$  defined by Eq. (A21) are approximately statistically independent whenever  $T \gg \tau_L$ .

### Appendix B: Likelihood Equations for the Three Parameters in Bullen Turbulence Spectra

In the case of the Bullen transverse and longitudinal three-parameter spectral forms,<sup>11</sup> Eq. (14) is replaced by

$$E\{S_j\} = \bar{S}_j = \sigma^2 L F_j(\ell, n), \quad j=1,2,\dots,N \quad (\text{B1})$$

which differs from Eq. (14) in that  $F_j$  is now a function of two parameters rather than one. Substituting Eq. (B1) into Eq. (13) yields instead of Eq. (15),

$$\begin{aligned} \ln[p(S_1, S_2, \dots, S_N)] = & - \left\{ N \ln(\sigma^2 L) + \ln F_1(\ell, n) \right. \\ & + \ln F_2(\ell, n) + \dots + \ln F_N(\ell, n) + \frac{1}{\sigma^2 L} \left[ \frac{S_1}{F_1(\ell, n)} \right. \\ & \left. \left. + \frac{S_2}{F_2(\ell, n)} + \dots + \frac{S_N}{F_N(\ell, n)} \right] \right\} \quad (\text{B2}) \end{aligned}$$

Differentiating Eq. (B2) with respect to the three parameters ( $\sigma^2 L$ ),  $\ell$ , and  $n$  and setting each of the resulting three expressions equal to zero yields, after minor manipulations, the three likelihood equations,

$$\sigma^2 L = \frac{1}{N} \sum_{j=1}^N \frac{S_j}{F_j(\ell, n)} \quad (\text{B3})$$

$$\sum_{j=1}^N G_{j\ell}(\ell, n) \left[ \frac{S_j}{F_j(\ell, n)} - \frac{1}{N} \sum_{i=1}^N \frac{S_i}{F_i(\ell, n)} \right] = 0 \quad (\text{B4})$$

$$\sum_{j=1}^N G_{jn}(\ell, n) \left[ \frac{S_j}{F_j(\ell, n)} - \frac{1}{N} \sum_{i=1}^N \frac{S_i}{F_i(\ell, n)} \right] = 0 \quad (\text{B5})$$

where

$$G_{j\ell}(\ell, n) \triangleq \frac{\partial}{\partial \ell} \ln F_j(\ell, n) \quad (\text{B6})$$

and

$$G_{jn}(\ell, n) \triangleq \frac{\partial}{\partial n} \ln F_j(\ell, n) \quad (\text{B7})$$

Equations (B3-B5) are the three-parameter spectrum counterparts to Eqs. (18) and (19). These likelihood equations are readily generalized to spectral forms containing any number of parameters by adding one additional equation of the same form as Eqs. (B4) and (B5) for each additional parameter in the function  $F_j(\cdot)$ .

The functions  $F_j(\ell, n)$ ,  $G_{j\ell}(\ell, n)$ , and  $G_{jn}(\ell, n)$  are,

for the Bullen transverse spectrum

$$F_j(\ell, n) = \frac{1 + 8\pi^2 \ell^2 k_j^2 (n+1)}{(1 + 4\pi^2 \ell^2 k_j^2)^{n+3/2}} \quad (\text{B8})$$

$$G_{j\ell}(\ell, n) = \frac{8\pi^2 \ell^2 k_j^2 (n+1/2)}{\ell} \times \left[ \frac{1 - 8\pi^2 \ell^2 k_j^2 (n+1)}{1 + 4\pi^2 \ell^2 k_j^2 (2n+3) + 32\pi^4 \ell^4 k_j^4 (n+1)} \right] \quad (\text{B9})$$

$$G_{jn}(\ell, n) = \frac{8\pi^2 \ell^2 k_j^2}{1 + 8\pi^2 \ell^2 k_j^2 (n+1)} - \ln(1 + 4\pi^2 \ell^2 k_j^2) \quad (\text{B10})$$

for the Bullen longitudinal spectrum

$$F_j(\ell, n) = \frac{2}{(1 + 4\pi^2 \ell^2 k_j^2)^{n+1/2}} \quad (\text{B11})$$

$$G_{j\ell}(\ell, n) = -\frac{1}{\ell} \frac{8\pi^2 \ell^2 k_j^2 (n+1/2)}{1 + 4\pi^2 \ell^2 k_j^2} \quad (\text{B12})$$

$$G_{jn}(\ell, n) = -\ln(1 + 4\pi^2 \ell^2 k_j^2) \quad (\text{B13})$$

For both the Bullen transverse and longitudinal spectra, the integral scale  $L$  is obtained from  $\ell$  and  $n$  by

$$L = \frac{\sqrt{\pi} \Gamma(n+1/2)}{\Gamma(n)} \ell \quad (\text{B14})$$

The Bullen transverse and longitudinal spectra obtained by combining Eq. (B1) with Eqs. (B8) and (B11), respectively, are two-sided spectra as in Eq. (28). Wave number  $k$  is in cycles/unit distance and  $L$  is the integral scale of the longitudinal spectrum, which is twice the integral scale of the transverse spectrum.<sup>11</sup>

From Eqs. (B1), (B8), and (B11), we can see that the parameter  $n$  governs the asymptotic slope of both the Bullen transverse and longitudinal spectra—when plotted on log-log coordinates the asymptotic slope of both spectra is  $-(2n+1)$ . When  $n=1/3$ , this asymptotic slope is  $-5/3$  and the Bullen forms reduce to the corresponding von Kármán forms.<sup>11</sup> When  $n=1/2$ , this asymptotic slope is  $-2$  and the Bullen forms reduce to the Dryden forms.<sup>11</sup>

For either the transverse or longitudinal case, as appropriate, the two likelihood equations (B4) and (B5) are to be solved simultaneously<sup>16</sup> for the parameters  $\ell$  and  $n$  by utilizing the periodogram samples  $S_1, S_2, \dots, S_N$  obtained from Eq. (29) and the values of  $k_j$  obtained from Eq. (30). Using these values of  $\ell$  and  $n$ , Eq. (B3) is then solved for  $\sigma^2 L$ , and Eq. (B14) is solved for  $L$ . The value of  $\sigma^2$  is obtained from the solution of Eq. (B3) as  $\sigma^2 = (\sigma^2 L)/L$ . The above solution method capitalizes on the invariance property<sup>14</sup> of maximum likelihood estimators.

### Acknowledgments

Support of this work by the National Aeronautics and Space Administration under Contract NAS1-14837 is gratefully acknowledged. Computer programming of the method leading to the results shown in Figs. 2-4 was carried out by Raymond W. Fischer of BBN with exceptional accuracy and efficiency. Support for writing of the paper was provided by the Bolt Beranek and Newman Science Development Program.

### References

- Lumley, J. L. and Panofsky, H. A., *The Structure of Atmospheric Turbulence*, Interscience/Wiley, New York, 1964.
- Houbolt, J. C., "Atmospheric Turbulence," *AIAA Journal*, Vol. 11, April 1973, pp. 421-437.



- <sup>3</sup>Etkin, B., "Turbulent Wind and Its Effect on Flight," *Journal of Aircraft*, Vol. 18, May 1981, pp. 327-345.
- <sup>4</sup>Davenport, W. B. Jr. and Root, W. L., *An Introduction to the Theory of Random Signals and Noise*, McGraw-Hill Book Co., New York, 1958.
- <sup>5</sup>Lin, C. C., *Statistical Theories of Turbulence*, Princeton University Press, Princeton, N. J., 1961, p. 43.
- <sup>6</sup>von Kármán, Th., "Progress in the Statistical Theory of Turbulence," *Proceedings of the National Academy of Sciences, USA*, Vol. 34, 1948, pp. 530-539.
- <sup>7</sup>Hinze, J. O., *Turbulence*, 2nd ed., McGraw-Hill Book Co., New York, 1975, pp. 244-253.
- <sup>8</sup>Tennekes, H. and Lumley, J. L., *A First Course in Turbulence*, MIT Press, Cambridge, Mass., 1972, Chap. 8.
- <sup>9</sup>Lumley, J. L., *Stochastic Tools in Turbulence*, Academic Press, New York, 1970.
- <sup>10</sup>Jones, J. W., Mielke, R. H., Jones, G. W., Gunter, G. E., and Monson, K. R., "Low Altitude Atmospheric Turbulence Lo-Loat Phase III, Vol. 1, Part 1, Data Analysis," AFFDL-TR-70-10, Nov. 1970.
- <sup>11</sup>Taylor, J., *Manual on Aircraft Loads*, Pergamon Press, Oxford, England, 1965, Chap. 9.
- <sup>12</sup>Kendall, M. G. and Stuart, A., *The Advanced Theory of Statistics*, 4th ed., Vol. 2, Macmillan, New York, 1979.
- <sup>13</sup>Kendall, M. G. and Stuart, A., *The Advanced Theory of Statistics*, 4th ed., Vol. 1, Macmillan, New York, 1977.
- <sup>14</sup>Freeman, H., *Introduction to Statistical Inference*, Addison-Wesley, Reading, Mass., 1963.
- <sup>15</sup>Cramér, H., *Mathematical Methods of Statistics*, Princeton University Press, Princeton, N. J., 1946.
- <sup>16</sup>Edwards, A. W. F., *Likelihood*, Cambridge University Press, Cambridge, England, 1972.
- <sup>17</sup>Woodward, P. M., *Probability and Information Theory, with Applications to Radar*, 2nd ed., Pergamon Press, Oxford, England, 1964.
- <sup>18</sup>Mark, W. D., "Characterization, Parameter Estimation, and Aircraft Response Statistics of Atmospheric Turbulence," NASA CR 3463, Sept. 1981.
- <sup>19</sup>Levin, M. J., "Power Spectrum Parameter Estimation," *IEEE Transactions on Information Theory*, Vol. IT-11, Jan. 1965, pp. 100-107.
- <sup>20</sup>Rhyné, R. H., Murrow, H. N., and Sidwell, K., "Atmospheric Turbulence Power Spectral Measurements to Long Wavelengths for Several Meteorological Conditions," *Aircraft Safety and Operating Problems*, NASA SP-416, 1976, pp. 271-286.
- <sup>21</sup>Papoulis, A., "Minimum-Bias Windows for High-Resolution Spectral Estimates," *IEEE Transactions on Information Theory*, Vol. IT-19, Jan. 1973, pp. 9-12.
- <sup>22</sup>Mark, W. D. and Fischer, R. W., "Investigation of the Effects of Nonhomogeneous (or Nonstationary) Behavior on the Spectra of Atmospheric Turbulence," NASA CR 2745, Oct. 1976.
- <sup>23</sup>Mark, W. D., "Statistics of Multipath Transmission of Finite Bandwidth Signals," *Journal of the Acoustical Society of America*, Vol. 52, July 1972, pp. 413-425.

*From the AIAA Progress in Astronautics and Aeronautics Series . . .*

## TRANSONIC AERODYNAMICS—v. 81

*Edited by David Nixon, Nielsen Engineering & Research, Inc.*

Forty years ago in the early 1940s the advent of high-performance military aircraft that could reach transonic speeds in a dive led to a concentration of research effort, experimental and theoretical, in transonic flow. For a variety of reasons, fundamental progress was slow until the availability of large computers in the late 1960s initiated the present resurgence of interest in the topic. Since that time, prediction methods have developed rapidly and, together with the impetus given by the fuel shortage and the high cost of fuel to the evolution of energy-efficient aircraft, have led to major advances in the understanding of the physical nature of transonic flow. In spite of this growth in knowledge, no book has appeared that treats the advances of the past decade, even in the limited field of steady-state flows. A major feature of the present book is the balance in presentation between theory and numerical analyses on the one hand and the case studies of application to practical aerodynamic design problems in the aviation industry on the other.

696 pp., 6×9, illus., \$30.00 Mem., \$55.00 List

TO ORDER WRITE: Publications Order Dept., AIAA, 1633 Broadway, New York, N.Y. 10019